



# Corrosion assessment of promising hydrated salts as sorption materials for thermal energy storage systems

Angel G. Fernández<sup>1</sup>, Margalida Fullana<sup>1,2</sup>, Luigi Calabrese<sup>3,4</sup>, Valeria Palomba<sup>4</sup>,  
Andrea Frazzica<sup>4</sup>, Luisa F. Cabeza<sup>1,\*</sup>

<sup>1</sup>GREiA Research Group, Universitat de Lleida, Pere de Cabrera s/n, 25001 Lleida, Spain

<sup>2</sup>CIRIAF-Interuniversity Research Centre on Pollution and Environment Mauro Felli, Via G. Duranti 63,  
06125, Perugia, Italy

<sup>3</sup>Department of Engineering, University of Messina, Messina, Italy

<sup>4</sup>CNR – ITAE – Istituto di Tecnologie Avanzate per l'Energia “Nicola Giordano”, Salita S. Lucia sopra  
Contesse 5, Messina 98126, Italy

\* Corresponding author: lcabeza@diei.udl.cat

## Abstract

Salt hydrates are an appealing option to be used as sorption materials in thermal energy storage (TES). In this work, strontium bromide and magnesium sulphate have been selected as one of the most promising salt hydrates since they present high energy storage density ( $>130$  kWh/m<sup>3</sup>) and efficiency ( $>20\%$ ). One of the main drawbacks of sorption materials rely on control the hydration-dehydration process but there are other parameters that can modify this behaviour as the corrosive potential of these salts in contact with the container material selected for the application. Hence, four different metal container materials, specifically stainless steel, copper, aluminium, and carbon steel have been tested in SrBr<sub>2</sub>·6H<sub>2</sub>O and MgSO<sub>4</sub>·7H<sub>2</sub>O hydrate salts, during 100 h at dehydration conditions. After the gravimetric and micrograph analysis carried out via scanning electron microscopy (SEM) study, only carbon steel is not recommended for this application in contact with SrBr<sub>2</sub>·6H<sub>2</sub>O, obtaining a corrosion rate of 0.038 mm/year, with a metallographic corrosion layer thickness of 25.2 microns. Aluminium, copper and stainless steel showed a better corrosion resistance also in SrBr<sub>2</sub>·6H<sub>2</sub>O and MgSO<sub>4</sub>·7H<sub>2</sub>O with corrosion rates below 0.008 mm/year.

**Keywords:** Sorption materials; hydrated salts; thermal energy storage; corrosion

## 1. Introduction

Society is making an effort to become less dependent on fossil fuel carbon-based energy sources to a more renewable and sustainable energy management. Efficient and sustainable energy systems should maximize the degree of energy decentralisation.

The buildings sector energy represents a 36% of the global energy consumption [1]. Currently, both space heating and cooling, as well as domestic hot water, are estimated to account for roughly half of global energy consumption in buildings [2]. To address this issue, thermal energy storage is a necessary technology that can adjust the mismatch of the supply and demand of thermal energy systems it can as well promote the independency of the energy grid and help reduce the building energy consumption. This specific thermal energy storage (TES) technology is meant to be used in mid-long term storage, i.e. exploit the solar thermal source in summer/day and releasing it in winter/night when the need is found, or else benefit from the heat waste of an industrial process.

The three ways of storing heat are by means of sensible, latent or sorption storage materials technologies depending on how this heat is stored [3]. Sorption heat storage has the possibility for a long-term storage at near ambient conditions and a higher energy density. According to Hadorn et al. [4], energy density in sorption materials using hydrated salts can reach  $185 \text{ kWh/m}^3$ , while in sensible and latent heat storage about it is about  $55 \text{ kWh/m}^3$  and  $94 \text{ kWh/m}^3$ , respectively. This storage potential relies on the reversible adsorption or absorption reactions, during which the energy is absorbed or released by breaking or reforming chemical or physical bonds.

N'Tsoukpoe et al. [5] made a multi-step screening of 125 salt hydrates to be used as sorption materials. The most promising materials found were  $\text{SrBr}_2 \cdot 6\text{H}_2\text{O}$  and  $\text{MgSO}_4 \cdot 7\text{H}_2\text{O}$ , since they present the highest energy storage density ( $>130 \text{ kWh/m}^3$ ) and efficiency ( $>20\%$ ).

Sorption materials for thermal energy storage have a minimum storage density of  $1 \text{ GJ/m}^3$  (depending on operating conditions) [6], avoiding heat losses during storage. Using salt hydrates, a storage volume of  $4\text{--}8 \text{ m}^3$  would be sufficient for the storage [7] of the energy needed for an average household for one year [8].

69 However, one of the main drawbacks that can modify this behaviour is the corrosion  
70 produced in the container materials due to it can introduce impurities in our system and  
71 change the hydration-dehydration reactions [9-11].

72 Few literature was found concerning the performance of salt hydrates corrosion on metals  
73 for sorption TES application. Cabeza et al. [12] analysed the corrosion behaviour of  
74 aluminium, brass, copper, carbon Steel and stainless steel in salt hydrate pairs in the range  
75 of 48 to 58°C. In this case the corrosive environment used was sodium acetate trihydrate  
76 and sodium trisulphate pentahydrate. Results showed that brass and copper should be  
77 avoided for long term immersion in the hydrated salts used.

78 D'Ans et al. [13] studied the corrosion produced by  $\text{SrBr}_2 \cdot 6\text{H}_2\text{O}$  in low carbon steel and  
79 copper at 80°C in different moisture conditions, 35 and 24%, respectively, during 30 days.  
80 Higher corrosion resistance was found in copper compared to carbon steel but in this case  
81 no vacuum pressure was applied inside the reactor, so  $\text{SrCO}_3$  corrosive impurities were  
82 formed.

83 Solé et al. [14] studied corrosion of aluminium, copper, stainless steel, and carbon steel  
84 immersed in  $\text{Na}_2\text{S}$ ,  $\text{CaCl}_2$ ,  $\text{MgCl}_2$ , and  $\text{Ca}(\text{OH})_2$  in a controlled humidity chamber for time  
85 periods of 1, 4, and 12 weeks. Tests were also performed for stainless steel and copper  
86 with coatings immersed for one week into  $\text{Na}_2\text{S} \cdot 9\text{H}_2\text{O}$  under vacuum [15]. Even though  
87 it might not be realistic to use pure salt hydrates for large scale implementation [16] and  
88 composites are being synthesised [17, 18] it is interesting to be aware of the nature and  
89 properties of the salts.

90 The present study analyses the corrosion resistance of aluminium, copper, carbon steel,  
91 and stainless steel immersed in  $\text{SrBr}_2 \cdot 6\text{H}_2\text{O}$  under vacuum pressure of 123 mbar and a  
92 temperature of 78 °C and  $\text{MgSO}_4 \cdot 7\text{H}_2\text{O}$  at 130°C and 20 mbar of vacuum pressure, during  
93 100 hours. These conditions correspond to their highest temperature during the  
94 dehydration process and the worst case scenario under operation conditions.

95

96

97

98

99

100

101

## 2. Materials and methods

### 2.1 Experimental set up

The corrosion test was performed at a self-built set-up composed by a closed jacketed reactor connected to a thermal bath as a heating unit providing the temperature and pressure necessary for each corrosive environment.

The set-up consists on a reactor where the beakers containing the salt hydrate and the immersed metal are placed (Figure 1). It is a 5 l jacketed reactor and through the external cylinder the thermal fluid (water or thermal oil, depending the testing temperature) is pumped from the heating unit (thermal bath), to control the reactor temperature, as well as the tube connected to the evaporator/condenser round bottom flask. The tubes connecting the heating unit to the reactor are PVC flexible tubes. The pressure inside the reactor is controlled by means of a vacuum pump PC 600 series from Vacuumbrand, which has its own refrigeration unit. The tubes connecting the vacuum pump to inner part of the reactor are polyamide-based.

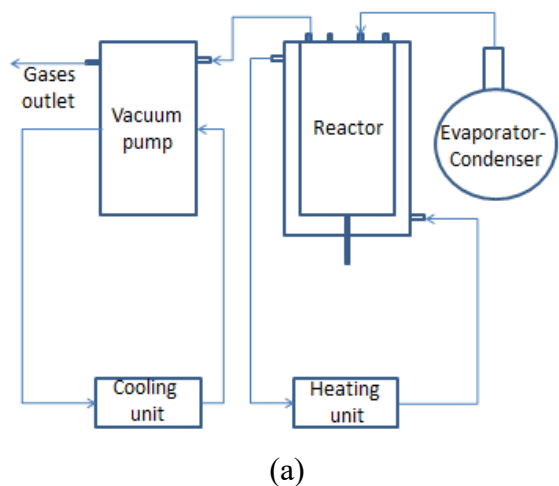


Figure 1. (a) Schema of the corrosion set-up. (b) Picture of the corrosion set-up.

The reactor is made of glass which is an inert material able to stand high temperatures and pressures. Furthermore, it allows direct visual inspection during the experiment. The

122 tubing and reactor were recovered with insulation to minimize thermal losses. The reactor  
 123 contains one open 300 ml vessel to place the sorption material (50g) and the specimens  
 124 to be tested.

125

126 **2.2 Materials**

127

128 The sorption materials tested in this study are SrBr<sub>2</sub>·6H<sub>2</sub>O and MgSO<sub>4</sub>·7H<sub>2</sub>O (Alfa Aesar,  
 129 99%).

130 The potential materials for the containers studied were stainless steel, copper, aluminium,  
 131 and carbon steel with the chemical composition shown in Table 1.

132

133

134

Table 1. Chemical composition of the metals tested

Material	Weight (%)									
	Al	Mn	Ni	Cr	P	C	S	Fe	Cu	Mo
<b>AISI 304</b>	-	1.7	8.04	18.28	-	-	-	Balance	-	0.27
<b>Carbon Steel (AISI 1090)</b>	-	0.6-0.9	-	-	0.04	0.85-0.98	0.05	Balance	-	-
<b>Aluminium</b>	100	-	-	-	-	-	-	-	-	-
<b>Copper</b>	-	-	-	-	-	-	-	-	100	-

135

136 The metal surface was polished with #600 SiC abrasive papers to avoid small defects that  
 137 can increase a localized corrosion. After this, coupons were washed with distilled water  
 138 and subsequently with acetone.

139

140 **2.3 Corrosion test methodology**

141

142 The salt was in powder form and studied in its hydrated state, using 50g per crucible. Two  
 143 50 cl beakers were placed inside the reactor (Figure 2). Each beaker contains enough  
 144 sorption material, salt hydrate, to allow the immersion of the metal coupons inside.

145

146

147

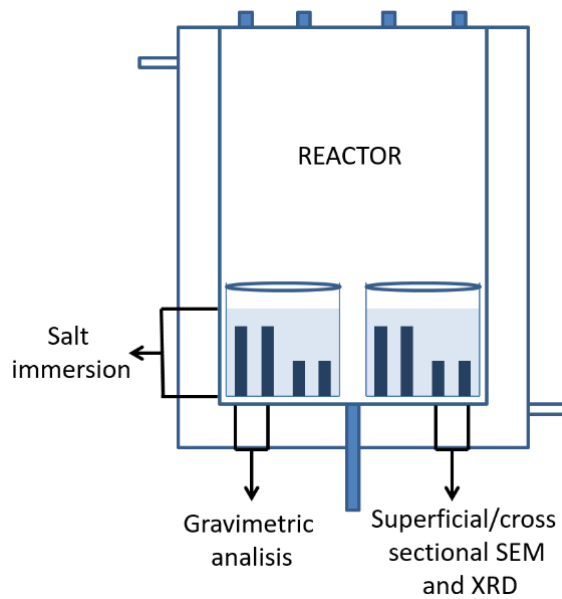


Figure 2. Metal coupons distribution inside the reactor beakers.

Four samples for each metal were studied, all of them had relatively similar thickness (0.5-1 mm). There were two larger samples (12 mm x 40 mm x 1 mm approx.) meant to be studied for the gravimetric analysis. The two smaller samples (12 mm x 15 mm x 1 mm approx.) were to be analysed visually by superficial or transversal scanning electronic microscope (SEM) and by X-ray diffraction (XRD) if necessary.

The metal specimens were prepared by cleaning their surface with paper rubbing or slight polishing in order to obtain a homogeneous surface. Afterwards, they were weighed in a precision balance ( $\pm 0.01$  mg) AG135 from Mettler-Toledo. The dimensions of each sample, in order to know the area that will be in contact with the molten salt, were also registered with a digital caliper ( $\pm 0.02$  mm).

Regarding the experimental conditions, the worst case scenario during the application of sorption materials is the dehydration step. This process involves higher temperatures and the realisation of water molecules which usually is related with corrosion processes. For  $\text{SrBr}_2 \cdot 6\text{H}_2\text{O}$  the temperature was set at  $78^\circ\text{C}$ ,  $10^\circ\text{C}$  below the melting of the salt  $88.6^\circ\text{C}$  [19] which must be prevented, using a vacuum pressure of 129 mbar to allow the dehydration process (Figure 3). The heating rate used was  $10^\circ\text{C}/\text{min}$  and the cooling mode after the corrosion test was slow ( $2^\circ\text{C}/\text{min}$ ) to avoid thermal stress in the samples.

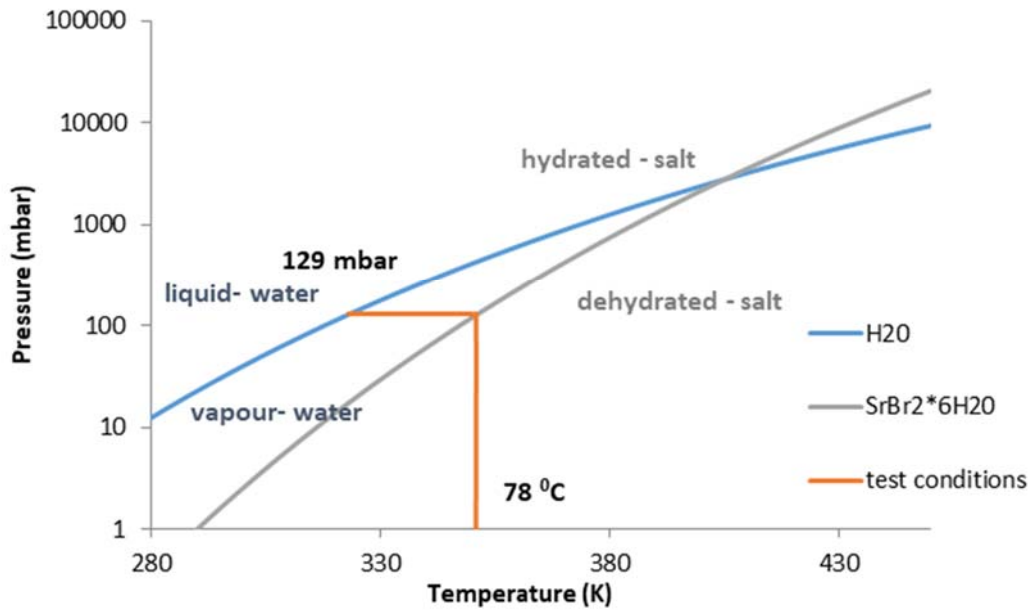


Figure 3. Test conditions: temperature of 78 °C and 129 mbar vacuum.

179

180

181

182 In order to create the equilibrium curves, the hydration-dehydration reaction (r) for the  
 183 salt (equation I) and change of state from liquid to vapour (L/G) for water (equation II),  
 184 the following equations were used:

185

$$P = \exp\left[\frac{-\Delta h_r}{R \cdot T} + \frac{\Delta S_r}{R}\right] \cdot P^0 \quad \text{Eq. I}$$

186

$$P = \exp\left[\frac{-\Delta h_{L/G}}{R \cdot T} + \frac{\Delta S_{L/G}}{R}\right] \cdot P^0 \quad \text{Eq. II}$$

187

188 where  $\Delta H$  is the enthalpy of the reaction or the state change, is the entropy  $\Delta S$  of the  
 189 reaction of the state change,  $R$  is the ideal gas constant,  $T$  is the temperature,  $P_0$  is the  
 190 normal pressure and  $P$  is the pressure corresponding the defined T.

191

192 On the other hand, the experimental conditions selected for corrosion test in  
 193  $\text{MgSO}_4 \cdot 7\text{H}_2\text{O}$  was 130°C and 20 mbar of vacuum pressure, in order to work at highest  
 194 temperature in dehydration conditions [5].

195

196 After corrosion tests, coupons are removed from the salt and cooled slowly. During the  
 197 drying (samples were cleaned after immersion using hot water in order to remove the salt  
 198 remaining) and handling process the specimen could present spallation and loss of the



199 corrosion layer, due the thermal expansion coefficient variation between the different  
200 oxides formed in the steel surface, producing non accurate values during the gravimetric  
201 test. In order to avoid this uncertainty, an evaluation of the weight loss is necessary. This  
202 method analyses the weight lost in the steel removing the corrosion layer produced after  
203 the corrosion process. The methodology to evaluate the corrosion proposed by the ASTM  
204 standard (G1-03) [21] is widely used in many fields. The procedure involves corroded  
205 metal immersed in a cleaning solution that reacts with the oxide layer depending on the  
206 nature of the base material; ASTM standard proposes different solutions and thermal  
207 treatments, removing only corrosion products.

208

209 Finally, the formula used to calculate the corrosion rate is:

210

$$211 \quad CR = \frac{\Delta m}{A \cdot (t_0 - t_f)}$$

212

213 where CR is the corrosion rate,  $\Delta m$  is the mass loss, A the contact area of the salt hydrate  
214 with the metal coupon and the time of exposure ( $t_0 - t_f$ ) in the corrosive environment.

215

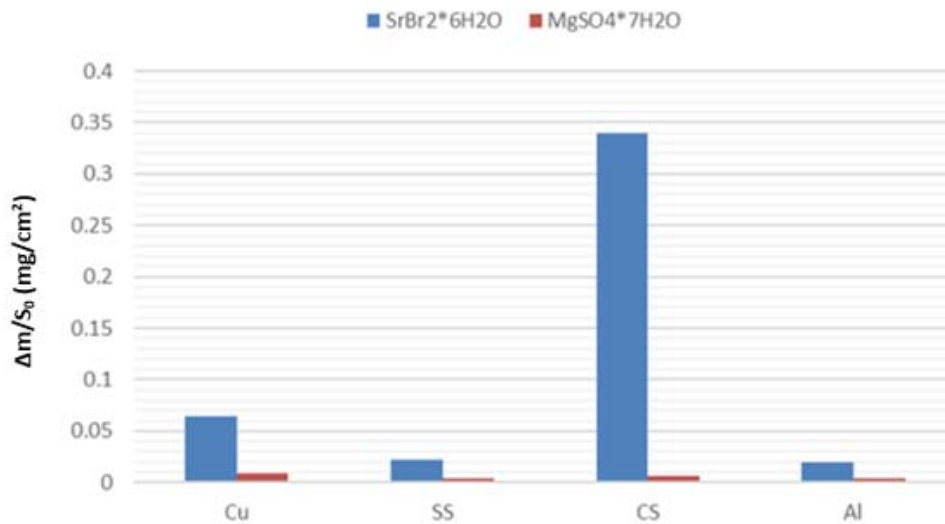
### 216 **3. Results**

217

218

219 The gravimetric values ( $\Delta m/S_o$ ) obtained in the materials tested are shown in Figure 4,  
220 after 100 hours of immersion in the sorption environments proposed.

221



222

223 Figure 4. Gravimetric values obtained for each material in the sorption materials tested

224

225 As it was shown in Figure 4, SrBr<sub>2</sub>·6H<sub>2</sub>O presents a higher corrosion behaviour and the  
 226 following gravimetric weight loss order can be established:

227

$$CS > Cu > SS = Al$$

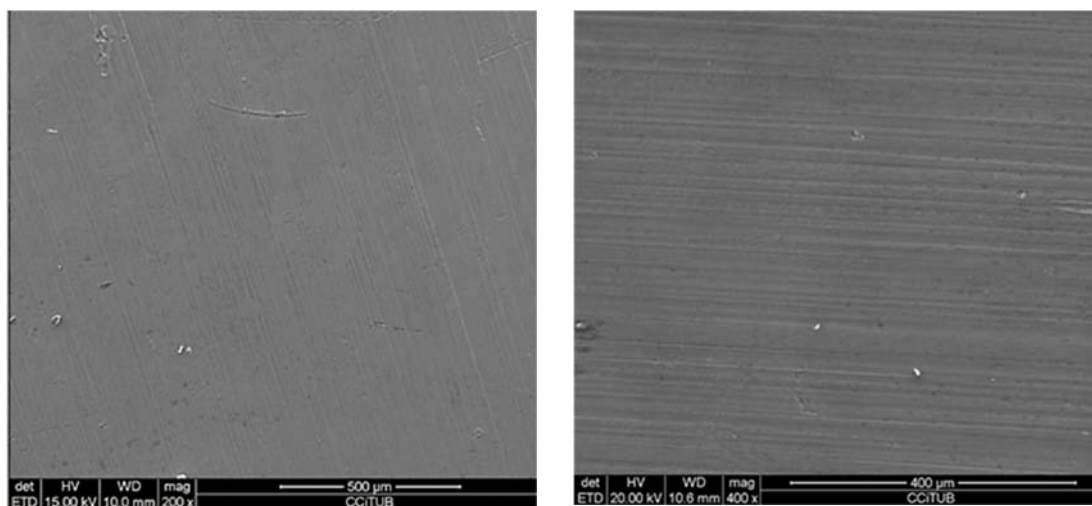
229

230 Aluminium showed high corrosion resistance in both sorption materials tested. Figure 5  
 231 shows the surface analysis performed by SEM in SrBr<sub>2</sub>·6H<sub>2</sub>O (left) and MgSO<sub>4</sub>·7H<sub>2</sub>O  
 232 (right). No corrosive products have been detected during 100 hours of immersion.

233

234

235



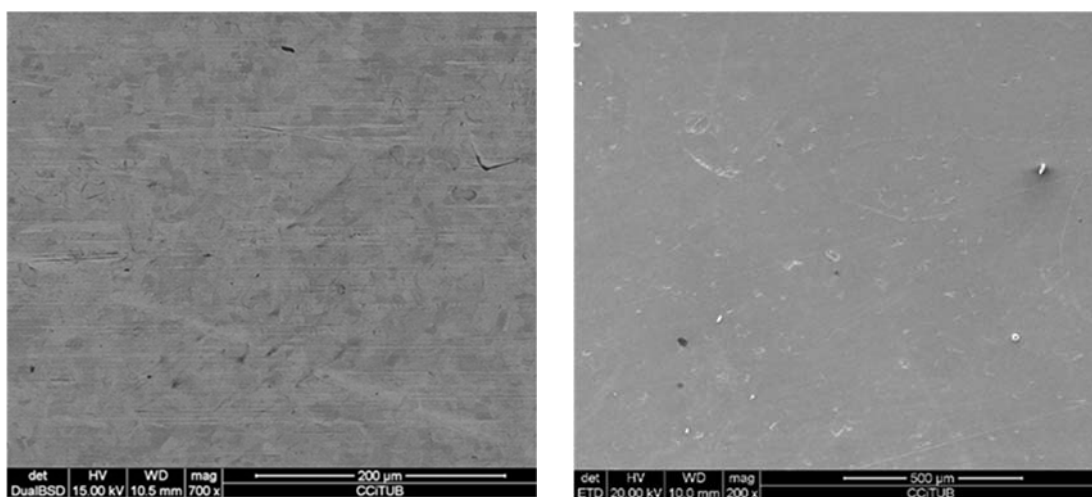
236 Figure 5. SEM superficial study of Aluminium immersed in SrBr<sub>2</sub>·6H<sub>2</sub>O (left) and  
 237 MgSO<sub>4</sub>·7H<sub>2</sub>O (right)

238

239

240 The stainless steel tested (AISI 304) showed a similar corrosion resistance compared  
 241 with the aluminium coupons, thus no corrosion products were detected in the steel  
 242 surface after the corrosion process (Figure 6).

243

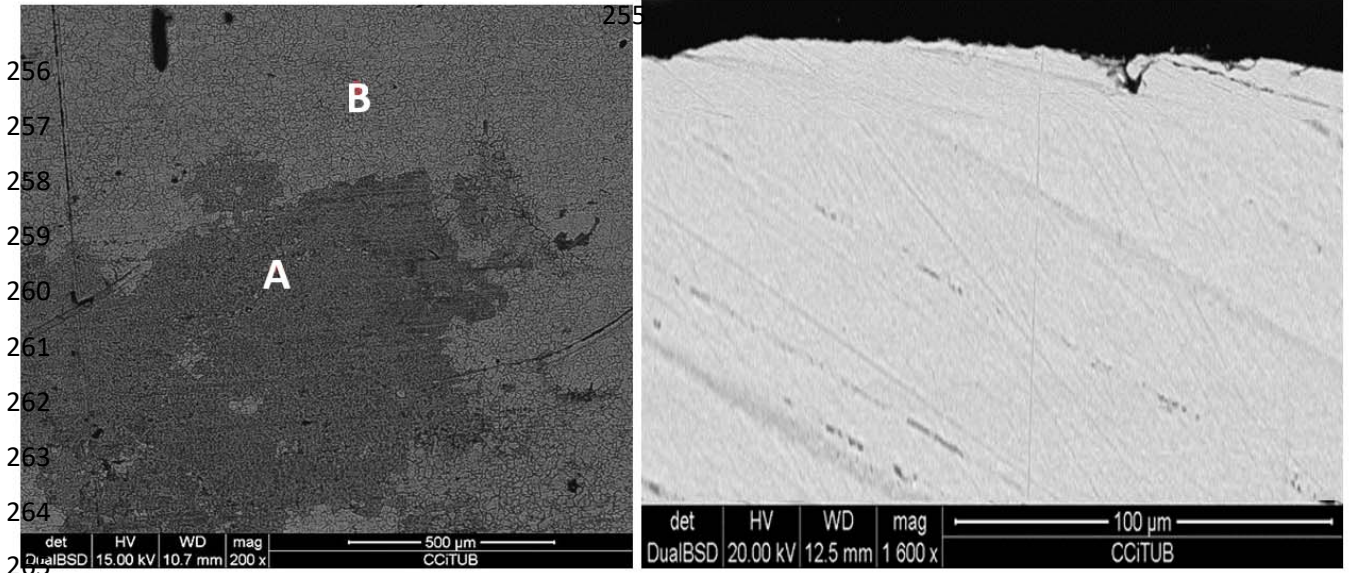


244 Figure 6. SEM superficial study of stainless steel immersed in SrBr<sub>2</sub>·6H<sub>2</sub>O (left) and  
 245 MgSO<sub>4</sub>·7H<sub>2</sub>O (right)

246

247 Higher corrosion behaviour was observed in copper coupons compared with aluminium  
 248 and stainless steel. This behaviour is higher when coppers is immersed in SrBr<sub>2</sub>·6H<sub>2</sub>O.  
 249 Figure 7 shows the superficial view (left) and the cross section study (right) after 100  
 250 hours at 78°C using a vacuum pressure of 129 mbar.

Spectro	Cu (wt.%)	O (wt.%)
A	94.04	5.96
B	96.75	3.25



266 Figure 7. Superficial (left) and cross section (right) study of  $\text{SrBr}_2 \cdot 6\text{H}_2\text{O}$  corrosion on  
 267 the copper coupons.

268

269 Superficial and transversal pictures showed a slight corrosion layer in the steel surface  
 270 with some content of copper oxide.

271 Better corrosion resistance was observed in  $\text{MgSO}_4 \cdot 7\text{H}_2\text{O}$  salt. Figure 8 shows the  
 272 superficial micrograph obtained.

273

274

275

276

277

278



279

280 Figure 8. SEM superficial study of copper immersed in  $\text{MgSO}_4 \cdot 7\text{H}_2\text{O}$  at  $130^\circ\text{C}$  and 20  
 281 mbar of vacuum pressure during 100 hours  
 282

283

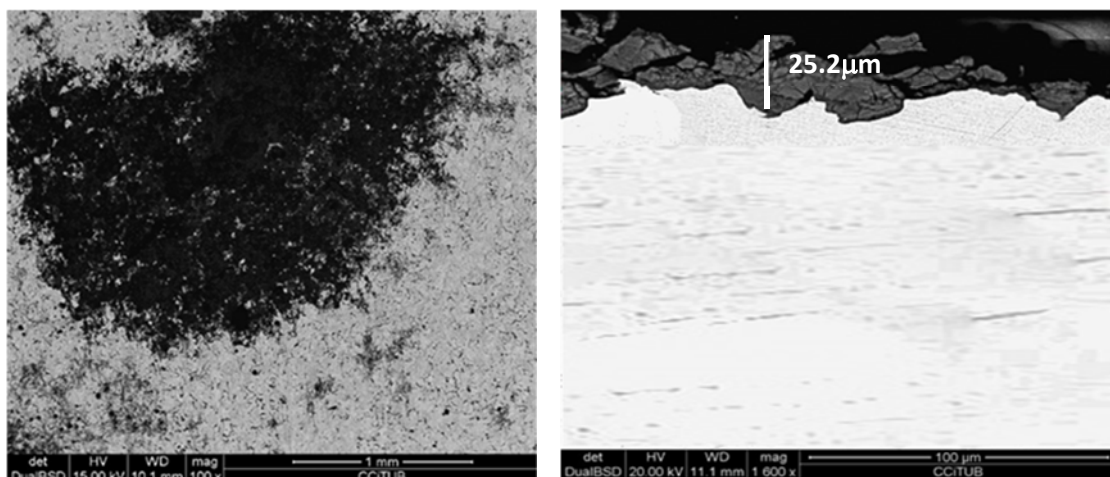
284

285 Carbon steel was the metal which showed the highest corrosion in contact with  
 286  $\text{SrBr}_2 \cdot 6\text{H}_2\text{O}$ .

287

288 The analysis of this metal was also observed via superficial (Figure 9 left) and cross  
 289 section (Figure 9 right) study. The corrosion layer thickness obtained was 27.5 microns.

289

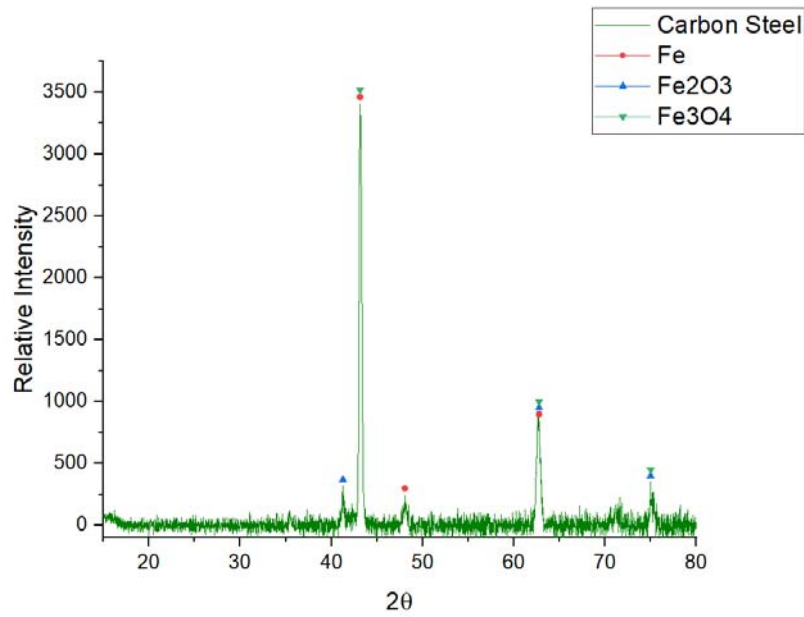


290 Figure 9. Superficial (left) and cross section (right) study of  $\text{SrBr}_2 \cdot 6\text{H}_2\text{O}$  corrosion on  
 291 the carbon steel coupons.  
 292

293

294 The composition of this corrosion layer was detected by XRD (Figure 10), obtaining  
 hematite ( $\text{Fe}_2\text{O}_3$ ) and magnetite ( $\text{Fe}_3\text{O}_4$ ) as the main corrosion products.

295



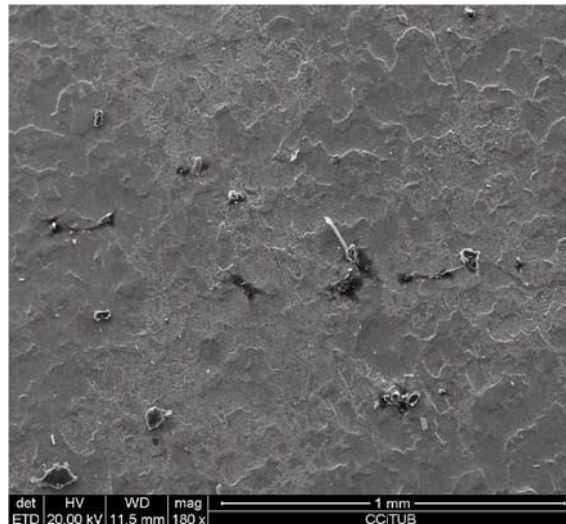
296

297 Figure 10. XRD analysis of the  $\text{SrBr}_2 \cdot 6\text{H}_2\text{O}$  corrosion on the carbon steel coupons.

298

As in the previous cases, the corrosion resistance of carbon steel in  $\text{MgSO}_4 \cdot 7\text{H}_2\text{O}$  was higher compared with the strontium bromide salt and no corrosion products were detected, just a few impurity particles were observed in the steel surface (Figure 11).

299



300

301 Figure 11. SEM superficial study of carbon steel immersed in  $\text{MgSO}_4 \cdot 7\text{H}_2\text{O}$  at 130°C

302

and 20 mbar of vacuum pressure during 100 hours

Finally, the corrosion rates for the materials tested in the different corrosive environments are presented in Table 2. Basing the suitability of the materials on the gravimetric analysis the most compatible metals are stainless steel and aluminium.

303

Experimental conditions inside the corrosion reactor shown in Figure 1, run in continuous mode and water vapour pressure is always as expected since it is taken from the external evaporator, which is also under vacuum. Corrosion rates in bromide salts are higher compared with hydrated magnesium sulphate salts tested, since they act as good ligands for iron with a low electronegativity. Adsorbed bromide ions also can interfere with the mechanism of anodic dissolution of iron, which may lead to an increase in the corrosion rate at higher concentrations of bromide ions.

In Table 3, a recommendation guide for the corrosion rates levels in industry is shown. According to this, carbon steel is not recommended for its use in contact with strontium bromide and copper should be use with caution, based on the specific application.

304

Table 2. Gravimetric and corrosion rate values for each metal after the immersion under  $\text{SrBr}_2 \cdot 6\text{H}_2\text{O}$  and  $\text{MgSO}_4 \cdot 7\text{H}_2\text{O}$

Metal	$\text{SrBr}_2 \cdot 6\text{H}_2\text{O}$		$\text{MgSO}_4 \cdot 7\text{H}_2\text{O}$	
	$\Delta m/S_o$ ( $\text{mg}/\text{cm}^2$ )	CR [ $\text{mm}/\text{yr}$ ]	$\Delta m/S_o$ ( $\text{mg}/\text{cm}^2$ )	CR [ $\text{mm}/\text{yr}$ ]
Aluminium	0.02	0.002	0.004	0.0004
Stainless steel	0.022	0.002	0.004	0.0004
Cu	0.064	0.008	0.009	0.001
Carbon Steel	0.34	0.038	0.006	0.0007

305

306

307

308 Table 3. Recommendation guide for corrosion rates CR in industry. Adapted from Ghali  
 309 et al. [20].

mg/cm <sup>2</sup> yr	mm/yr	Recommendation
> 1000	2	Completely destroyed with
100 to 999	0.2 – 1.99	Not recommended for service greater than a month
50 to 99	0.1 – 0.19	Not recommended for service greater than one year
10 to 49	0.02 – 0.09	Caution recommended, based on the specific application
0.3 to 9.9	-	Recommended for long term service
< 0.2	-	Recommended for long term service; no corrosion, only as a result of cleaning

310

311 Materials compatibility under real operation conditions was analysed, obtaining a good  
 312 performance for copper, stainless steel and aluminium coupons in both sorption materials  
 313 tested. Carbon steel showed a higher gravimetric weight loss and Fe<sub>2</sub>O<sub>3</sub> and Fe<sub>3</sub>O<sub>4</sub> were  
 314 detected in the steel surface. The formation of these corrosive compounds can modify the  
 315 reactions involved in the hydrate-dehydrate reactions forming intermediate compounds  
 316 in the corrosive environments. This behaviour was not detected in the screening material  
 317 tests carried out in this research but the interaction between corrosion products and water  
 318 molecules would be taken into account in future researches in this topic.

319

320

#### 321 4. Conclusions

322

323 A self-built set-up composed by a closed and integrated 5 l jacketed reactor, a thermal  
 324 bath as a heating unit and a vacuum pump to control the pressure, has been designed for  
 325 proper corrosion studies in sorption materials.

326

327 The sorption materials tested in this study were SrBr<sub>2</sub>·6H<sub>2</sub>O and MgSO<sub>4</sub>·7H<sub>2</sub>O, analysing  
 328 their corrosion behaviour at dehydration conditions on different hypothetical container  
 329 materials such as stainless steel (SS), copper (Cu), aluminium (Al), and carbon steel (CS).  
 330 After having analysed the results it can be concluded that carbon steel is not a suitable  
 331 candidate in contact with SrBr<sub>2</sub>·6H<sub>2</sub>O, since it showed a corrosion rate of 0.038 mm/year.



332 Superficial and cross sectional study by SEM also detected a corrosion layer of 27.5  
333 microns, where  $\text{Fe}_2\text{O}_3$  and  $\text{Fe}_3\text{O}_4$  were identified by XRD. Copper showed a lower  
334 corrosion rate 0.008 mm/year in  $\text{SrBr}_2 \cdot 6\text{H}_2\text{O}$ , but this material should be used with  
335 caution, based on the specific application. The best performance was obtained from the  
336 aluminium and the stainless steel coupons which almost didn't show a visual change and  
337 had a corrosion rate of 0.002 mm/year.

338 On the other hand, materials tested in  $\text{MgSO}_4 \cdot 7\text{H}_2\text{O}$  salt showed a low corrosion rate and  
339 they are recommended as contained materials using magnesium sulphate heptahydrated  
340 as thermal energy storage material.

341 This research establishes the first experimental corrosion studies in sorption materials  
342 under vacuum pressure, avoiding interaction with atmospheric compounds that can react  
343 with the inorganic sorption salts affecting the hydration-dehydration kinetic process  
344 and reducing the corrosion resistance in the container material.

345

#### 346 **Acknowledgements**

347

348 This work was partially funded by the Ministerio de Ciencia, Innovación y Universidades  
349 de España (RTI2018-093849-B-C31 - MCIU/AEI/FEDER, UE). The authors would like  
350 to thank the Catalan Government for the quality accreditation given to their research  
351 group GREiA (2017 SGR 1537). GREiA is a certified agent TECNIO in the category of  
352 technology developers from the Government of Catalonia. This work is partially  
353 supported by ICREA under the ICREA Academia programme.

354

355

#### 356 **References**

357

358 [1] Buildings, (n.d.). <https://www.iea.org/topics/energyefficiency/buildings/>  
359 (accessed 1 April 2019).

360 [2] IEA webstore. Technology Roadmap - Energy-Efficient Buildings - Heating and  
361 Cooling Equipment, (n.d.). [https://webstore.iea.org/technology-roadmap-energy-](https://webstore.iea.org/technology-roadmap-energy-efficient-buildings-heating-and-cooling-equipment)  
362 [efficient-buildings-heating-and-cooling-equipment](https://webstore.iea.org/technology-roadmap-energy-efficient-buildings-heating-and-cooling-equipment) (accessed 1 April 2019).

363 [3] H. Ibrahim, A. Ilinca, J. Perron, Energy storage systems—Characteristics and  
364 comparisons, *Renew. Sustain. Energy Rev.* 12 (2008) 1221–1250.

365 [4] J. C. Hadorn, G. Berney -Base, 009-Advanced storage concepts for active solar

- 366 energy IEA-SHC Task 32 2003-2007 Operating agent Task 32 for the Swiss  
367 Federal Office of Energy, n.d. <http://www.iea-shc.org/> (accessed 4 April 2019).
- 368 [5] K.E. N'Tsoukpoe, T. Schmidt, H.U. Rammelberg, B.A. Watts, W.K.L. Ruck, A  
369 systematic multi-step screening of numerous salt hydrates for low temperature  
370 thermochemical energy storage, *Appl. Energy*. 124 (2014) 1–16.
- 371 [6] H. Lahmidi, S. Mauran, V. Goetz, Definition, test and simulation of a  
372 thermochemical storage process adapted to solar thermal systems, *Sol. Energy*. 80  
373 (2006) 883–893.
- 374 [7] B. Michel, N. Mazet, P. Neveu, Experimental investigation of an innovative  
375 thermochemical process operating with a hydrate salt and moist air for thermal  
376 storage of solar energy: Global performance, *Appl. Energy*. 129 (2014) 177–186.
- 377 [8] S. Mauran, H. Lahmidi, V. Goetz, Solar heating and cooling by a thermochemical  
378 process. First experiments of a prototype storing 60kWh by a solid/gas reaction,  
379 *Sol. Energy*. 82 (2008) 623–636.
- 380 [9] A. Fopah-Lele, J.G. Tamba, A review on the use of  $\text{SrBr}_2 \cdot 6\text{H}_2\text{O}$  as a potential  
381 material for low temperature energy storage systems and building applications,  
382 *Sol. Energy Mater. Sol. Cells*. 164 (2017) 175–187.
- 383 [10] A. Fopah-Lele, C. Rohde, K. Neumann, T. Tietjen, T. Rönnebeck, K.E.  
384 N'Tsoukpoe, T. Osterland, O. Opel, W.K.L. Ruck, Lab-scale experiment of a  
385 closed thermochemical heat storage system including honeycomb heat exchanger,  
386 *Energy*. 114 (2016) 225–238.
- 387 [11] H. U. Rammelberg, T. Osterland, B. Priehs, O. Opel, W. K.L. Ruck,  
388 Thermochemical heat storage materials-performance of mixed salt hydrates. 2016,  
389 *Solar Energy* 136, pp: 571–589
- 390 [12] L.F. Cabeza, J. Roca, M. Nogues, H. Mehling, S. Hiebler. Immersion corrosion  
391 tests on metal-salt hydrate pairs used for latent heat storage in the 48 to 58°C  
392 temperature range. 2002, *Materials and corrosion*, 53, pp: 902-907.
- 393 [13] P. D'Ansa, E. Courbon, M. Frère, G. Descy, T. Segato, M. Degrez, Severe  
394 corrosion of steel and copper by strontium bromide in thermochemical heat storage  
395 reactors. 2018, *corrosion science*, 138, pp: 275-283.
- 396 [14] A. Solé, L. Miró, C. Barreneche, I. Martorell, L.F. Cabeza, Corrosion of metals  
397 and salt hydrates used for thermochemical energy storage, *Renew. Energy*. 75  
398 (2015) 519–523.
- 399 [15] A. Solé, C. Barreneche, I. Martorell, L.F. Cabeza, Corrosion evaluation and

- 400 prevention of reactor materials to contain thermochemical material for thermal  
401 energy storage, *Appl. Therm. Eng.* 94 (2016) 355–363.
- 402 [16] P.A.J. Donkers, L.C. Sögütöglu, H.P. Huinink, H.R. Fischer, O.C.G. Adan, A  
403 review of salt hydrates for seasonal heat storage in domestic applications, *Appl.*  
404 *Energy*. 199 (2017) 45–68.
- 405 [17] V. Brancato, L. Calabrese, V. Palomba, A. Frazzica, M. Fullana-Puig, A. Solé, L.F.  
406 Cabeza, MgSO<sub>4</sub>·7H<sub>2</sub>O filled macro cellular foams: An innovative composite  
407 sorbent for thermo-chemical energy storage applications for solar buildings, *Sol.*  
408 *Energy*. 173 (2018) 1278–1286.
- 409 [18] Y.J. Zhao, R.Z. Wang, Y.N. Zhang, N. Yu, Development of SrBr<sub>2</sub> composite  
410 sorbents for a sorption thermal energy storage system to store low-temperature  
411 heat, *Energy*. 115 (2016) 129–139.
- 412 [19] W.M. Haynes, D.R. Lide, T.J. Bruno, *CRC handbook of chemistry and physics : a*  
413 *ready-reference book of chemical and physical data.*, CRC Press, 2016.
- 414 [20] E. Ghali S.Vedula, E. Sastri, M. Elboujdaini, *Corrosion prevention and protection :*  
415 *practical solutions*, Wiley, 2007. [https://www.wiley.com/en-](https://www.wiley.com/en-us/Corrosion+Prevention+and+Protection%3A+Practical+Solutions-p-9780470024027)  
416 [us/Corrosion+Prevention+and+Protection%3A+Practical+Solutions-p-](https://www.wiley.com/en-us/Corrosion+Prevention+and+Protection%3A+Practical+Solutions-p-9780470024027)  
417 [9780470024027](https://www.wiley.com/en-us/Corrosion+Prevention+and+Protection%3A+Practical+Solutions-p-9780470024027) (accessed 19 November 2018).
- 418 [21] International, ASTM G1-03 Standard practice for preparing, cleaning, and  
419 evaluating corrosion test specimens. Annual Book of ASTM standards, section 3,  
420 Metal test methods and analytical procedures, American Society for Testing and  
421 Materials (ASTM) 2003.

422  
423  
424